MULTIDIMENSIONAL SUMMATION-BY-PARTS OPERATORS: GENERAL THEORY AND APPLICATION TO SIMPLEX ELEMENTS[*]

JASON E. HICKEN[†], DAVID C. DEL REY FERNÁNDEZ[‡], AND DAVID W. ZINGG[‡]

Abstract. Summation-by-parts (SBP) finite-difference discretizations share many attractive properties with Galerkin finite-element methods (FEMs), including time stability and superconvergent functionals; however, unlike FEMs, SBP operators are not completely determined by a basis, so the potential exists to tailor SBP operators to meet different objectives. To date, application of high-order SBP discretizations to multiple dimensions has been limited to tensor product domains. This paper presents a definition for multidimensional SBP finite-difference operators that is a natural extension of one-dimensional SBP operators. Theoretical implications of the definition are investigated for the special case of a diagonal-norm (mass) matrix. In particular, a diagonal-norm SBP operator exists on a given domain if and only if there is a cubature rule with positive weights on that domain and the polynomial-basis matrix has full rank when evaluated at the cubature nodes. Appropriate simultaneous-approximation terms are developed to impose boundary conditions weakly, and the resulting discretizations are shown to be time stable. Concrete examples of multidimensional SBP operators are constructed for the triangle and tetrahedron; similarities and differences between these SBP operators and those typically used in spectral-element, spectral-difference, and nodal discontinuous Galerkin methods are discussed. An assembly process is described that builds SBP operators on a global domain from element-level operators. Numerical results of linear advection on a doubly periodic domain demonstrate the accuracy and time stability of the simplex operators.

Key words. summation-by-parts, finite-difference method, unstructured grid, spectral-element method, spectral-difference method, mimetic discretization

AMS subject classifications. 65N06, 65M60, 65N12

DOI. 10.1137/15M1038360

1. Introduction. Summation-by-parts (SBP) operators are high-order finite-difference schemes that mimic the symmetry properties of the differential operators they approximate [23]. Respecting such symmetries has important implications; in particular, they enable SBP discretizations that are both time stable and high-order accurate [5, 37, 30], properties that are essential for robust, long-time simulations of turbulent flows [28, 38].

Most existing SBP operators are one-dimensional [33, 27, 34, 26] and are applied to multidimensional problems using a multiblock tensor-product formulation [35, 18, 32]. Like other tensor-product methods, the restriction to multiblock grids complicates mesh generation and adaptation, and it limits the geometric complexity that can be considered in practice.

The limitations of the tensor-product formulation motivate our interest in generalizing SBP operators to unstructured grids. There are two ways this generalization has been pursued in the literature: (1) construct global SBP operators on an arbitrary distribution of nodes, or (2) construct SBP operators on reference elements and assemble a global discretization by coupling these smaller elements.

[†]Department of Mechanical, Aerospace, and Nuclear Engineering, Rensselaer Polytechnic Institute, Troy, NY 12180 (hickej2@rpi.edu).

[‡]Institute for Aerospace Studies, University of Toronto, Toronto, ON, M3H 5T6, Canada (dcdelrey @gmail.com, dwz@oddjob.utias.utoronto.ca).

The first approach is appealing conceptually, and it is certainly viable for second-order accurate SBP schemes. For example, Nordström et al. [31] showed that the vertex-centered second-order accurate finite-volume scheme[1] has a multidimensional SBP property, even on unstructured grids; however, the first approach presents challenges when constructing high-order operators. Kitson, McLachlan, and Robidoux [21] showed that, for a given stencil width and design accuracy, there exist grids for which no stable, diagonal-norm SBP operator exists. Thus, building stable high-order SBP operators on arbitrary node distributions may require unacceptably large stencils. When SBP operators do exist for a given node distribution, in general, they must be determined globally by solving a system of equations. The global nature of these SBP operators is exemplified in the mesh-free framework of Chiu and colleagues [6, 7].

The second approach—constructing SBP operators on reference elements and using these to build the global discretization—is more common and presents fewer difficulties. The primary challenge here is to extend the one-dimensional SBP operators of Kreiss and Scherer [23] to a broader set of operators and domains. The existence of such operators, at least in the dense-norm case,[2] was established by Carpenter and Gottlieb [3]. They proved that operators with the SBP property can be constructed from the Lagrangian interpolant on nearly arbitrary nodal distributions, which is practically feasible on reference elements with relatively few nodes. More recently, Gassner [13] showed that the discontinuous spectral-element method is equivalent to a diagonal-norm SBP discretization when the Legendre–Gauss–Lobatto nodes are used with a lumped mass matrix.

Of particular relevance to the present work is the extension of the SBP concept by Del Rey Fernández, Boom, and Zingg [10]. They introduced a generalized summation-by-parts (GSBP) definition for arbitrary node distributions on one-dimensional elements, and these ideas helped shape the definition of SBP operators presented herein.

Our first objective in the present work is to develop a suitable definition for multidimensional SBP operators on arbitrary grids and to characterize the resulting operators theoretically. We note that the discrete-derivative operator presented in [6] is a possible candidate for defining (diagonal-norm) multidimensional SBP operators; however, it lacks properties of conventional SBP operators that we would like to retain, such as the accuracy of the discrete divergence theorem [19].

Our second objective is to provide a concrete example of multidimensional diagonal-norm SBP operators on non–tensor-product domains. We focus on diagonal-norm operators because they are better suited to discretizations that conserve non-quadratic invariants [21]; they are also more attractive than dense norms for explicit time-marching schemes. We construct diagonal-norm SBP operators for triangular and tetrahedral elements. The resulting operators are similar to those used in the nodal triangular-spectral-element method [8, 29, 14]. Unlike the spectral-element method based on cubature points, the SBP method is not completely specified by a polynomial basis; we use the resulting freedom to enforce the SBP property, which leads to provably time-stable schemes.

The remaining paper is structured as follows. Section 2 presents notation and the proposed definition for multidimensional SBP operators. We study the theoretical implications of the proposed definition in section 3. We then describe, in section 4,

---

[1]On simplices, the vertex-centered finite-volume scheme is equivalent to a mass-lumped $p = 1$ finite-element discretization.

[2]In this paper, norm matrix is synonymous with mass matrix.

how to construct diagonal-norm SBP operators for the triangle and tetrahedron. Section 4 also establishes that SBP operators on subdomains can be assembled into SBP operators on the global domain. Results of applying the triangular SBP operators to the linear advection equation are presented in section 5. Conclusions are given in section 6.

2. Preliminaries. To make the presentation concise, we concentrate on multidimensional SBP operators in two dimensions; the extension to higher dimensions follows in a straightforward manner. Furthermore, we present definitions and theorems for operators in the x coordinate direction only; the corresponding definitions and theorems for the y coordinate direction follow directly from those in the x direction.

2.1. Notation. We consider discretized derivative operators defined on a set of n nodes, $S = \{(x_i, y_i)\}_{i=1}^n$. Capital letters with script type are used to denote continuous functions. For example, $\mathcal{U}(x) \in L^2(\Omega)$ denotes a square-integrable function on the domain Ω. We use the lowercase bold font to denote the restriction of functions to the nodes. Thus, the restriction of $\mathcal{U}$ to S is given by

$$\boldsymbol{u} = [\mathcal{U}(x_1, y_1), \ldots, \mathcal{U}(x_n, y_n)]^{\mathrm{T}}.$$

Several theorems and proofs make use of the monomial basis. For two spatial variables, the size of the polynomial basis of total degree p is

$$n_p^* \equiv \frac{(p+1)(p+2)}{2}.$$

More generally, $n_p^* = \binom{p+d}{d}$, where d is the spatial dimension. We use the following single-subscript notation for monomial basis functions:

$$\mathcal{P}_k(x, y) \equiv x^i y^{j-i}, \qquad k = j(j+1)/2 + i + 1 \quad \forall j \in \{0, 1, \ldots, p\}, \quad i \in \{0, 1, \ldots, j\}.$$

We will frequently evaluate $\mathcal{P}_k$ and $\partial \mathcal{P}_k / \partial x$ at the nodes S, so we introduce the notation

$$\boldsymbol{p}_k \equiv [\mathcal{P}_k(x_1, y_1), \ldots, \mathcal{P}_k(x_n, y_n)]^{\mathrm{T}}$$

$$\text{and} \qquad \boldsymbol{p}_k' \equiv \left[\frac{\partial \mathcal{P}_k}{\partial x}(x_1, y_1), \ldots, \frac{\partial \mathcal{P}_k}{\partial x}(x_n, y_n)\right]^{\mathrm{T}}.$$

Finally, matrices are represented using capital letters with sans serif font; for example, the first-derivative operators with respect to x and y are represented by the matrices D_x and D_y, respectively. Entries of a matrix are indicated with subscripts, and we follow MATLAB-like notation when referencing submatrices. For example, $\mathsf{A}_{:,j}$ denotes the jth column of matrix A, and $\mathsf{A}_{:,1:k}$ denotes its first k columns.

2.2. Multidimensional SBP operator definition. We propose the following definition for D_x, the SBP first-derivative operator with respect to x. An analogous definition holds for D_y and, in three-dimensions, D_z. A version of Definition 2.1 was first put forward in [9] and is a natural extension of the GSBP definition [10], which itself extends the classical SBP definition of Kreiss and Scherer [23].

DEFINITION 2.1 (two-dimensional SBP operator). *Consider an open and bounded domain $\Omega \subset \mathbb{R}^2$ with a piecewise-smooth boundary Γ. The matrix D_x is a degree p SBP approximation to the first derivative $\frac{\partial}{\partial x}$ on the nodes $S = \{(x_i, y_i)\}_{i=1}^n$ if*

1. $\mathsf{D}_x\boldsymbol{p}_k = \boldsymbol{p}'_k$ *for all* $k \in \{1, 2, \dots, n^*_p\}$;
2. $\mathsf{D}_x = \mathsf{H}^{-1}\mathsf{Q}_x$, *where* H *is symmetric positive definite; and*
3. $\mathsf{Q}_x = \mathsf{S}_x + \frac{1}{2}\mathsf{E}_x$, *where* $\mathsf{S}^{\mathrm{T}}_x = -\mathsf{S}_x$, $\mathsf{E}^{\mathrm{T}}_x = \mathsf{E}_x$, *and* E_x *satisfies*

$$\boldsymbol{p}^{\mathrm{T}}_k\mathsf{E}_x\boldsymbol{p}_m = \oint_\Gamma \mathcal{P}_k\mathcal{P}_m n_x \mathrm{d}\Gamma \qquad \forall\, k, m \in \{1, 2, \dots, n^*_\tau\},$$

where $\tau \geq p$ *and* n_x *is the* x *component of* $\boldsymbol{n} = [n_x, n_y]^{\mathrm{T}}$, *the outward pointing unit normal on* Γ.

Before studying the implications of Definition 2.1 in section 3, it is worthwhile to motivate and elaborate on the three properties in the definition.

Property 1 ensures that D_x is an accurate approximation to the first partial derivative with respect to x. The operator must be exact for polynomials of total degree less than or equal to p, so at least n^*_p nodes are necessary to satisfy property 1.

Remark 1. We emphasize that a polynomial basis is not used to define the solution in SBP methods, in contrast with the piecewise polynomial expansions found in FEMs. We adopt the monomial basis only to define the accuracy conditions concisely and avoid cumbersome Taylor-series expansions.

The matrix H must be symmetric positive definite to guarantee stability: without property 2, the discrete "energy," $\boldsymbol{u}^{\mathrm{T}}\mathsf{H}\boldsymbol{u}$, could be negative when $\boldsymbol{u}^{\mathrm{T}}\boldsymbol{u} > 0$, and vice versa. The so-called norm matrix H can be interpreted as a mass matrix, i.e.,

$$\mathsf{H}_{i,j} = \int_\Omega \phi_i(x, y)\phi_j(x, y)\mathrm{d}\Omega,$$

but it is important to emphasize that SBP operators are finite-difference operators, and there is no (known) closed-form expression for an SBP nodal basis $\{\phi_i\}^n_{i=1}$ in general. In the diagonal-norm case, we shall show that another interpretation of H is as a cubature rule.

Property 3 is needed to mimic integration by parts (IBP). Recall that the IBP formula for the x derivative is

$$\int_\Omega \mathcal{V}\frac{\partial\mathcal{U}}{\partial x}\mathrm{d}\Omega + \int_\Omega \mathcal{U}\frac{\partial\mathcal{V}}{\partial x}\mathrm{d}\Omega = \oint_\Gamma \mathcal{V}\mathcal{U}n_x\mathrm{d}\Gamma.$$

The discrete version of the IBP formula, which follows from property 3, is

$$\boldsymbol{v}^{\mathrm{T}}\mathsf{H}\mathsf{D}_x\boldsymbol{u} + \boldsymbol{u}^{\mathrm{T}}\mathsf{H}\mathsf{D}_x\boldsymbol{v} = \boldsymbol{v}^{\mathrm{T}}\mathsf{E}_x\boldsymbol{u} \qquad \forall\, \boldsymbol{v}, \boldsymbol{u} \in \mathbb{R}^n.$$

There is a one-to-one correspondence between each term in the IBP formula and its SBP proxy. For example, it is clear from property 3 that $\boldsymbol{v}^{\mathrm{T}}\mathsf{E}_x\boldsymbol{u}$ approximates the surface integral in IBP to order $\tau + 1$. Moreover, in section 3 we show that diagonal-norm SBP operators also approximate the left-hand side of IBP.

3. Analysis of diagonal-norm, multidimensional, SBP operators. In this section, we determine the implications of Definition 2.1 on the constituent matrices of a multidimensional SBP operator and whether or not such operators exist. We also investigate the time stability of discretizations based on multidimensional SBP operators. The focus is on diagonal-norm operators because (i) they are better suited to conserving nonquadratic quantities for nonlinear stability [21], and (ii) dense-norm operators, i.e., where the matrix H is not diagonal, do not appear to offer significant advantages over conventional FEMs.

The following lemma will prove useful in what follows. It follows immediately from properties 1 and 3, so we state it without proof.

LEMMA 3.1 (compatibility). *Let* $\mathsf{D}_x = \mathsf{H}^{-1}(\mathsf{S}_x + \frac{1}{2}\mathsf{E}_x)$ *be an SBP operator of degree* p. *Then we have the following set of relations:*

$$(3.1) \qquad \boldsymbol{p}_m^{\mathrm{T}}\mathsf{H}\boldsymbol{p}_k' + \boldsymbol{p}_k^{\mathrm{T}}\mathsf{H}\boldsymbol{p}_m' = \boldsymbol{p}_m^{\mathrm{T}}\mathsf{E}_x\boldsymbol{p}_k \qquad \forall\, k, m \in \{1, 2, \ldots, n_p^*\}.$$

We refer to (3.1) as the compatibility equations for the x derivative; H must simultaneously satisfy analogous relations for E_y. The relation between H and E_x was first derived by Kreiss and Scherer [23] and Strand [33] to construct a theory for one-dimensional classical finite-difference SBP operators. Furthermore, Del Rey Fernández, Boom, and Zingg [10] have used these relations to extend the theory of such operators to a broader set. What is presented in this paper is a natural extension of those works to multidimensional operators, and the derivation of (3.1) follows in a straightforward manner from any of the mentioned works.

Our first use of the compatibility equations is to prove that, in the diagonal-norm case, the multidimensional SBP definition conceals a cubature rule with positive weights.

THEOREM 3.2. *Let* $\mathsf{D}_x = \mathsf{H}^{-1}\mathsf{Q}_x$ *be a degree* p, *diagonal-norm, multidimensional SBP operator on the domain* Ω. *Then the nodes* $S = \{(x_i, y_i)\}_{i=1}^n$ *and the diagonal entries of* H *form a degree* $2p - 1$ *cubature rule on* Ω.

Proof. Using property 3 of Definition 2.1, the compatibility equations become

$$\sum_{j=1}^n \mathsf{H}_{j,j} \left[\mathcal{P}_m \frac{\partial \mathcal{P}_k}{\partial x} + \mathcal{P}_k \frac{\partial \mathcal{P}_m}{\partial x} \right]_{(x_j, y_j)} = \oint_\Gamma \mathcal{P}_m \mathcal{P}_k n_x \mathrm{d}\Gamma \qquad \forall\, k, m \in \{1, 2, \ldots, n_p^*\}.$$

Using the chain rule on the left and IBP on the right results in

$$(3.2) \qquad \sum_{j=1}^n \mathsf{H}_{j,j} \left. \frac{\partial \mathcal{P}_m \mathcal{P}_k}{\partial x} \right|_{(x_j, y_j)} = \int_\Omega \frac{\partial \mathcal{P}_m \mathcal{P}_k}{\partial x} \mathrm{d}\Omega \qquad \forall\, k, m \in \{1, 2, \ldots, n_p^*\}.$$

Since $\mathcal{P}_k$ and $\mathcal{P}_m$ are monomials of degree at most p, it follows that $\partial \left(\mathcal{P}_m \mathcal{P}_l \right) / \partial x$ is a scaled monomial of degree at most $2p - 1$; thus, by considering all of the combinations of k and m, (3.2) implies

$$\sum_{j=1}^n \mathsf{H}_{j,j} \mathcal{P}_k \left(x_j, y_j \right) = \int_\Omega \mathcal{P}_k \mathrm{d}\Omega \qquad \forall\, k \in \{1, 2, \ldots, n_{2p-1}^*\},$$

which are the conditions for a degree $2p - 1$ cubature. $\qquad\qquad \square$

We now prove one of our central theoretical results, relating the existence of a diagonal-norm SBP operator to the existence of a cubature rule with positive weights.

THEOREM 3.3. *Consider the node set* $S = \{(x_i, y_i)\}_{i=1}^n$ *with* $n \geq n_p^*$ *nodes, and define the generalized Vandermonde matrix* $\mathsf{V} \in \mathbb{R}^{n \times n_p^*}$ *whose columns are the monomial basis evaluated at the nodes:*

$$\mathsf{V}_{:,k} = \boldsymbol{p}_k \qquad \forall\, k \in \{1, 2, \ldots, n_p^*\}.$$

Assume that the columns of V *are linearly independent. Then the existence of a cubature rule of degree at least* $2p - 1$ *with positive weights on* S *is necessary and sufficient for the existence of degree* p *diagonal-norm SBP operators approximating the first derivatives* $\frac{\partial}{\partial x}$ *and* $\frac{\partial}{\partial y}$ *on the node set* S.

Proof. The necessary condition on H follows immediately from Theorem 3.2. To prove sufficiency, we must show that, given a cubature rule, we can construct an operator that satisfies properties 1–3 of Definition 2.1 on the same node set as the cubature rule.

Before proceeding, we introduce some matrices that facilitate the proof. Let $\mathsf{V}_x \in \mathbb{R}^{n \times n_p^*}$ be the matrix whose columns are the x derivatives of the monomial-basis:

$$(\mathsf{V}_x)_{:,k} = \boldsymbol{p}_k' \qquad \forall\, k \in \{1, 2, \ldots, n_p^*\}.$$

We construct an invertible matrix $\tilde{\mathsf{V}} \in \mathbb{R}^{n \times n}$ by appending a set of vectors, $\mathsf{W} \in \mathbb{R}^{n \times (n - n_p^*)}$, that are linearly independent among themselves and to the vectors in V:

$$\tilde{\mathsf{V}} \equiv \begin{bmatrix} \mathsf{V} & \mathsf{W} \end{bmatrix}.$$

Similarly, we define

$$\tilde{\mathsf{V}}_x \equiv \begin{bmatrix} \mathsf{V}_x & \mathsf{W}_x \end{bmatrix},$$

where $\mathsf{W}_x \in \mathbb{R}^{n \times (n - n_p^*)}$ is a matrix that will be specified later. Below, we use the degrees of freedom in W_x to satisfy the SBP definition.

Let H be the diagonal matrix whose entries are the cubature weights ordered consistently with the cubature node set S. Since the cubature weights are positive, property 2 is satisfied.

Next, we use the cubature to construct a suitable E_x. Using V and V_x, we define the symmetric matrix

$$(3.3) \qquad \tilde{\mathsf{E}}_x \equiv \mathsf{V}^{\mathrm{T}} \mathsf{H} \mathsf{V}_x + \mathsf{V}_x^{\mathrm{T}} \mathsf{H} \mathsf{V}.$$

Since V and V_x are polynomials of degree p and $p - 1$, respectively, evaluated at the nodes, the cubature is exact for the right-hand side of (3.3):

$$(3.4) \qquad \left(\tilde{\mathsf{E}}_x\right)_{k,m} = \int_\Omega \frac{\partial \mathcal{P}_k}{\partial x} \mathcal{P}_m \mathrm{d}\Omega + \int_\Omega \mathcal{P}_k \frac{\partial \mathcal{P}_m}{\partial x} \mathrm{d}\Omega = \oint_\Gamma \mathcal{P}_k \mathcal{P}_m n_x \mathrm{d}\Gamma$$

for all $k, m \in \{1, 2, \ldots, n_p^*\}$. Now we can define the boundary operator

$$\mathsf{E}_x \equiv \tilde{\mathsf{V}}^{-\mathrm{T}} \begin{bmatrix} \tilde{\mathsf{E}}_x & \mathsf{F}_x^{\mathrm{T}} \\ \mathsf{F}_x & \mathsf{G}_x \end{bmatrix} \tilde{\mathsf{V}}^{-1},$$

where $\mathsf{F}_x \in \mathbb{R}^{(n - n_p^*) \times n_p^*}$ and $\mathsf{G}_x = \mathsf{G}_x^{\mathrm{T}} \in \mathbb{R}^{(n - n_p^*) \times (n - n_p^*)}$. It follows from this definition that E_x is symmetric. Moreover, together with (3.4), this definition implies

$$\left(\mathsf{V}^{\mathrm{T}} \mathsf{E}_x \mathsf{V}\right)_{k,m} = \left(\tilde{\mathsf{E}}_x\right)_{k,m} = \oint_\Gamma \mathcal{P}_k \mathcal{P}_m n_x \mathrm{d}\Gamma \qquad \forall\, k, m \in \{1, 2, \ldots, n_p^*\},$$

so E_x satisfies the accuracy condition of property 3.

Finally, let

$$(3.5) \qquad \mathsf{S}_x \equiv \mathsf{H} \tilde{\mathsf{V}}_x \tilde{\mathsf{V}}^{-1} - \frac{1}{2} \mathsf{E}_x.$$

The accuracy conditions, which are equivalent to showing $\mathsf{D}_x \mathsf{V} = \mathsf{V}_x$, follow immediately from this definition of S_x:

$$\mathsf{D}_x \mathsf{V} = \mathsf{H}^{-1} \left(\mathsf{S}_x + \frac{1}{2} \mathsf{E}_x\right) \mathsf{V} = \mathsf{H}^{-1} \left(\mathsf{H} \tilde{\mathsf{V}}_x \tilde{\mathsf{V}}^{-1}\right) \mathsf{V} = \mathsf{V}_x;$$

thus, property 1 is satisfied.

Our remaining task is to show that S_x can be constructed to be antisymmetric. If we can show that

$$\tilde{\mathsf{V}}^{\mathrm{T}}\mathsf{S}_x\tilde{\mathsf{V}} = \begin{bmatrix} \mathsf{V}^{\mathrm{T}}\mathsf{S}_x\mathsf{V} & \mathsf{V}^{\mathrm{T}}\mathsf{S}_x\mathsf{W} \\ \mathsf{W}^{\mathrm{T}}\mathsf{S}_x\mathsf{V} & \mathsf{W}^{\mathrm{T}}\mathsf{S}_x\mathsf{W} \end{bmatrix}$$

can be made antisymmetric, then the result will follow for S_x. Consider the first block in the 2×2 block matrix above, i.e.,

$$\mathsf{V}^{\mathrm{T}}\mathsf{S}_x\mathsf{V} = \mathsf{V}^{\mathrm{T}}\mathsf{H}\mathsf{V}_x - \frac{1}{2}\mathsf{V}^{\mathrm{T}}\mathsf{E}_x\mathsf{V}.$$

Adding this block to its transpose, we find

$$(3.6) \qquad \mathsf{V}^{\mathrm{T}}\mathsf{S}_x\mathsf{V} + \mathsf{V}^{\mathrm{T}}\mathsf{S}_x^{\mathrm{T}}\mathsf{V} = \mathsf{V}^{\mathrm{T}}\mathsf{H}\mathsf{V}_x + \mathsf{V}_x^{\mathrm{T}}\mathsf{H}\mathsf{V} - \mathsf{V}^{\mathrm{T}}\mathsf{E}_x\mathsf{V},$$

where we have used the symmetry of E_x. The right-hand side of (3.6) is the matrix form of the (rearranged) compatibility equations (3.1). Thus, $\mathsf{V}^{\mathrm{T}}\mathsf{S}_x\mathsf{V} + \mathsf{V}^{\mathrm{T}}\mathsf{S}_x^{\mathrm{T}}\mathsf{V} = 0$, proving that the first block is antisymmetric. For the remaining three blocks, antisymmetry requires

$$\left(\mathsf{V}^{\mathrm{T}}\mathsf{S}_x\mathsf{W}\right)^{\mathrm{T}} = -\mathsf{W}^{\mathrm{T}}\mathsf{S}_x\mathsf{V} \qquad \text{and} \qquad \mathsf{W}^{\mathrm{T}}\mathsf{S}_x\mathsf{W} = -\mathsf{W}^{\mathrm{T}}\mathsf{S}_x^{\mathrm{T}}\mathsf{W}.$$

Substituting S_x and E_x and simplifying, we obtain the following equations:

$$(3.7) \qquad \mathsf{W}_x^{\mathrm{T}}\mathsf{H}\mathsf{V} + \mathsf{W}^{\mathrm{T}}\mathsf{H}\mathsf{V}_x = \mathsf{F}_x \qquad \text{and} \qquad \mathsf{W}^{\mathrm{T}}\mathsf{H}\mathsf{W}_x + \mathsf{W}_x^{\mathrm{T}}\mathsf{H}\mathsf{W} = \mathsf{G}_x.$$

The two matrix equations above constitute $n(n - n_p^*)$ scalar equations. We are free to choose W_x, G_x, and F_x, so the matrix equations are underdetermined (W_x alone has $n(n - n_p^*)$ entries). To prove existence of an SBP operator we need only find one solution; for example, take $\mathsf{W}_x = 0$, $\mathsf{G}_x = 0$, and $\mathsf{F}_x = \mathsf{W}^{\mathrm{T}}\mathsf{H}\mathsf{V}_x$. Thus, the equations can be satisfied to ensure the antisymmetry of S_x. $\qquad\square$

Remark 2. In general, there are infinitely many operators associated with a given cubature rule that satisfy Definition 2.1. For example, the proof of Theorem 3.3 only considered one way to solve (3.7). Another way to satisfy these conditions is to set $\mathsf{F}_x = 0$ and then solve

$$\left(\mathsf{V}^{\mathrm{T}}\mathsf{H}\right)\mathsf{W}_x = -\mathsf{V}_x^{\mathrm{T}}\mathsf{H}\mathsf{W}$$

for W_x by finding the minimum Frobenius-norm solution. G_x can then be computed directly from the second equation in (3.7).

Remark 3. The requirement that V be full rank is similar to, but less stringent than, the unisolvency condition [1]. The latter requires the Vandermonde matrix to be invertible on the nodes, which is challenging to satisfy if the nodes are also required to be a cubature rule. In contrast, Theorem 3.3 permits $n \geq n_p^*$, and this expands the set of cubatures that are suitable for a given polynomial degree at the expense of increasing the number of degrees of freedom.

The following theorem characterizes the matrices Q_x and S_x in terms of the bilinear forms that they approximate. The theorem is useful when discretizing the weak form of a PDE, rather than the strong form, using SBP finite-difference operators.

THEOREM 3.4. *Let* $\mathsf{D}_x = \mathsf{H}^{-1}\mathsf{Q}_x = \mathsf{H}^{-1}\left(\mathsf{S}_x + \frac{1}{2}\mathsf{E}_x\right)$ *be a diagonal-norm SBP operator of degree p on the domain* Ω. *Then*

$$(3.8) \qquad \boldsymbol{p}_k^{\mathrm{T}}\mathsf{Q}_x\boldsymbol{p}_m = \int_\Omega \mathcal{P}_k\frac{\partial\mathcal{P}_m}{\partial x}\mathrm{d}\Omega,$$

$$(3.9) \qquad \boldsymbol{p}_k^{\mathrm{T}}\mathsf{S}_x\boldsymbol{p}_m = \int_\Omega \mathcal{P}_k\frac{\partial\mathcal{P}_m}{\partial x}\mathrm{d}\Omega - \frac{1}{2}\oint_\Gamma \mathcal{P}_k\mathcal{P}_m n_x\mathrm{d}\Gamma,$$

where $k, m \leq n_\tau^*$ *and* $\mathcal{P}_k\mathcal{P}_m$ *is at most degree* $2p$.

Proof. The proof of (3.8) is analogous to the proof in [19] for one-dimensional classical finite-difference SBP operators. With (3.8) established, we can substitute $\mathsf{Q}_x = \mathsf{S}_x + \frac{1}{2}\mathsf{E}_x$ and rearrange to obtain

$$\boldsymbol{p}_k^{\mathrm{T}}\mathsf{S}_x\boldsymbol{p}_m = \int_\Omega \mathcal{P}_k\frac{\partial\mathcal{P}_m}{\partial x}\mathrm{d}\Omega - \frac{1}{2}\boldsymbol{p}_k^{\mathrm{T}}\mathsf{E}_x\boldsymbol{p}_m = \int_\Omega \mathcal{P}_k\frac{\partial\mathcal{P}_m}{\partial x}\mathrm{d}\Omega - \frac{1}{2}\oint_\Gamma \mathcal{P}_k\mathcal{P}_m n_x\mathrm{d}\Gamma,$$

where we have used the accuracy property of E_x to get the desired result. $\qquad\square$

3.1. Stability analysis. We conclude our analysis of diagonal-norm multidimensional SBP operators by investigating the stability of an SBP semidiscretization of the constant-coefficient advection equation

$$(3.10) \qquad \begin{aligned} \frac{\partial\mathcal{U}}{\partial t} + \beta_x\frac{\partial\mathcal{U}}{\partial x} + \beta_y\frac{\partial\mathcal{U}}{\partial y} &= 0 \qquad \forall\,(x, y) \in \Omega, \\ \mathcal{U}(x, y, t) &= \mathcal{U}_{\mathrm{bc}}(x, y, t) \qquad \forall\,(x, y) \in \Gamma_-, \end{aligned}$$

where $\Gamma^- = \{(x, y) \in \Gamma \mid \beta_x n_x + \beta_y n_y < 0\}$ is the inflow boundary and $\Gamma^+ = \Gamma \setminus \Gamma^-$ is the outflow boundary.

Let D_x and D_y be SBP operators and let E_x and E_y be their corresponding boundary operators. In order to impose the boundary conditions in a stable manner, we introduce the decomposition

$$(3.11) \qquad \beta_x\mathsf{E}_x + \beta_y\mathsf{E}_y = \mathsf{E}_+ + \mathsf{E}_-,$$

where E_+ is symmetric positive semidefinite and E_- is symmetric negative semidefinite, and

$$\boldsymbol{p}_k^{\mathrm{T}}\mathsf{E}_\pm\boldsymbol{p}_m = \oint_{\Gamma_\pm} \mathcal{P}_k\mathcal{P}_m\left(\beta_x n_x + \beta_y n_y\right)\mathrm{d}\Gamma \qquad \forall\,k, m \in \{1, 2, \ldots, n_\tau^*\}.$$

The existence of the decomposition (3.11) is guaranteed, provided that $\mathsf{F}_x = \mathsf{F}_y = 0$; see Appendix A for the proof.

Using D_x and D_y and the matrix E_-, a consistent semidiscretization of (3.10) is given by

$$(3.12) \qquad \frac{d\boldsymbol{u}}{dt} + \beta_x\mathsf{D}_x\boldsymbol{u} + \beta_y\mathsf{D}_y\boldsymbol{u} = \sigma\mathsf{H}^{-1}\mathsf{E}_-\left(\boldsymbol{u} - \boldsymbol{u}_{\mathrm{bc}}\right).$$

The three terms on the left-hand side of (3.12) correspond to the three terms in the strong form of the PDE. The terms on the right-hand side of (3.12) are penalties that enforce the boundary conditions weakly using simultaneous-approximation terms (SATs) [12, 4]. The boundary data is supplied by the vector $\boldsymbol{u}_{\mathrm{bc}}$, which must produce a sufficiently accurate reconstruction of $\mathcal{U}_{\mathrm{bc}}$ along the boundary. Evaluating $\mathcal{U}_{\mathrm{bc}}$

is adequate when the nonzeros of E_x correspond to nodes that lie on Γ, such as the simplex operators presented below. More generally, a preprocessing step can be performed to find a suitable $\boldsymbol{u}_{\mathrm{bc}}$.

We now show that (3.12) is time stable.

THEOREM 3.5. *Let $\boldsymbol{u}$ be the solution to* (3.12) *with homogeneous boundary conditions and bounded initial condition. Then the norm* $\|\boldsymbol{u}\|_{\mathsf{H}} = \sqrt{\boldsymbol{u}^{\mathrm{T}} \mathsf{H} \boldsymbol{u}}$ *is nonincreasing if* $\sigma \geq \frac{1}{2}$.

Proof. Multiplying the semidiscretization (with $\boldsymbol{u}_{\mathrm{bc}} = \boldsymbol{0}$) from the left by $\boldsymbol{u}^{\mathrm{T}} \mathsf{H}$, we find

$$\boldsymbol{u}^{\mathrm{T}} \mathsf{H} \frac{d\boldsymbol{u}}{dt} + \beta_x \boldsymbol{u}^{\mathrm{T}} \mathsf{Q}_x \boldsymbol{u} + \beta_y \boldsymbol{u}^{\mathrm{T}} \mathsf{Q}_y \boldsymbol{u} = \sigma \boldsymbol{u}^{\mathrm{T}} \mathsf{E}_- \boldsymbol{u}$$

$$\Rightarrow \quad \frac{d\|\boldsymbol{u}\|_{\mathsf{H}}^2}{dt} = -\boldsymbol{u}^{\mathrm{T}} \mathsf{E}_+ \boldsymbol{u} + (2\sigma - 1) \boldsymbol{u}^{\mathrm{T}} \mathsf{E}_- \boldsymbol{u}.$$

To obtain the last line, we used the definitions of Q_x and Q_y, as well as the decomposition (3.11). The first quadratic form on the right is nonpositive by definition of E_+. The result follows if $\sigma \geq \frac{1}{2}$, since E_- is negative semidefinite. □

4. Constructing the operators. This section describes how we construct diagonal-norm SBP operators for triangles and tetrahedra. The algorithms described below have been implemented in the Julia package SummationByParts.[3]

4.1. The node coordinates and the norm matrix. Theorem 3.2 tells us that the diagonal entries in H are positive weights from a cubature that is exact for polynomials of total degree $2p - 1$. Thus, our first task is to find cubature rules with positive weights for the triangle and tetrahedron. Additionally, we seek rules that use as few nodes as possible for a given order of accuracy while respecting the symmetries of the triangle and tetrahedron; the former condition is for efficiency, while the latter condition is to reduce directional biases.

For the operators considered in this paper, we require that $\binom{p+d-1}{d-1}$ cubature nodes lie on each boundary facet, where d is the spatial dimension. This requirement on the nodes is motivated by the particular form of the E_x, E_y, and E_z operators that we consider below; however, Definition 2.1 does not require a prescribed number of boundary nodes, and SBP operators for the 2- and the 3-simplex exist that do not have any boundary nodes at all. In this case the E matrices still obey property 3 of Definition 2.1, but they must also have a particular symmetric decomposition to ensure boundary and interface data can be imposed in a stable manner; this decomposition is the subject of a forthcoming paper.

Cubature rules that meet our requirements for triangular elements are presented in references [24, 8, 29, 14] in the context of the spectral-element (SE) and spectral-difference (SD) methods. Table 1 summarizes the rules that are adopted for triangular-element SBP operators of degree $p = 1, 2, 3$, and 4. For reference, the node locations for the triangular cubature rules are shown in Figure 1.

To find cubature rules for the tetrahedron, we follow the ideas presented in [14, 39, 36]. Our procedure is briefly outlined below for completeness, but we make no claims regarding the novelty of the cubature rules nor our method of finding them.

We assume that each node belongs to a (possibly degenerate) symmetry orbit [39]. As indicated above, we assume that the cubature node set includes $p + 1$ nodes along

---

[3]See https://github.com/OptimalDesignLab/SummationByParts.jl.

TABLE 1
Active orbits and their node counts for triangular-element operators. The notation Perm *indicates that every permutation of the barycentric coordinates is to be considered. Free-node counts are decomposed into the product of the number of nodes in the orbit times the number of orbits of that type.*

			Operator degree, p			
	Orbit name	Barycentric form	1	2	3	4
Fixed nodes	vertices	Perm$(1, 0, 0)$	3	3	3	3
	mid-edge	Perm $\left(\frac{1}{2}, \frac{1}{2}, 0\right)$	—	3	—	3
	centroid	$\left(\frac{1}{3}, \frac{1}{3}, \frac{1}{3}\right)$	—	1	—	—
Free nodes	edge	Perm $(\alpha, 1 - \alpha, 0)$	—	—	6×1	6×1
	S_{21}	Perm $(\alpha, \alpha, 1 - 2\alpha)$	—	—	3×1	3×2
		# free parameters	—	—	2	3
		# nodes total	3	7	12	18
		cubature degree	1	3	5	7

$p = 1$ $p = 2$ $p = 3$ $p = 4$
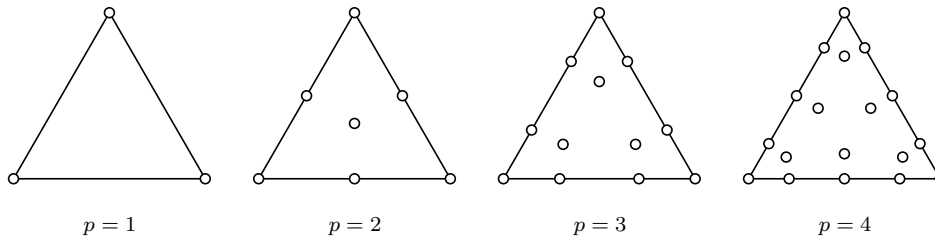
FIG. 1. *Node distributions for cubature rules adopted for the SBP operators on triangles.*

each edge and $(p+1)(p+2)/2$ nodes on each triangular face. For the interior nodes, we activate the minimum number of symmetry orbits necessary to satisfy the accuracy conditions; these orbits have been identified through trial and error.

Each symmetry orbit has a cubature weight associated with it, and orbits that are nondegenerate are parameterized using one or more barycentric parameters. Together, the orbit parameters and the weights are the degrees of freedom that must be determined. They are found by solving the nonlinear accuracy conditions using the Levenberg–Marquardt algorithm. The accuracy conditions are implemented using the integrals of orthogonal polynomials on the tetrahedron [22, 11].

Table 2 summarizes the node sets used for the tetrahedron cubature rules, and Figure 2 illustrates the node coordinates.

4.2. The boundary operators. Definition 2.1 implies that the boundary operator E_x satisfies

$$\boldsymbol{v}^{\mathrm{T}} \mathsf{E}_x \boldsymbol{u} = \oint_\Gamma \mathcal{U} \mathcal{V} n_x \, d\Gamma$$

for all polynomials $\mathcal{U}$ and $\mathcal{V}$ whose total degree is less than $\tau \geq p$. In particular, if we choose $\mathcal{U}$ and $\mathcal{V}$ to be nodal basis functions on the faces, we can isolate the entries of E_x. This is possible because we have insisted on operators with $\binom{p+d-1}{d-1}$ nodes on each facet, which leads to a complete nodal basis. For further details on the construction of the boundary operators, we direct the interested reader to [16, p. 187].

TABLE 2
Active orbits and their node counts for tetrahedral-element operators. See the caption of Table 1 for an explanation of the notation.

	Orbit name	Barycentric form	Operator degree, p			
			1	2	3	4
Fixed nodes	vertices	$\mathsf{Perm}(1,0,0,0)$	4	4	4	4
	mid-edge	$\mathsf{Perm}\left(\frac{1}{2},\frac{1}{2},0,0\right)$	—	6	—	6
	centroid	$\left(\frac{1}{4},\frac{1}{4},\frac{1}{4},\frac{1}{4}\right)$	—	1	—	1
	face centroid	$\mathsf{Perm}\left(\frac{1}{3},\frac{1}{3},\frac{1}{3},0\right)$	—	—	4	—
Free nodes	edge	$\mathsf{Perm}\left(\alpha,1-\alpha,0,0\right)$	—	—	12×1	12×1
	face S_{21}	$\mathsf{Perm}\left(\alpha,\alpha,1-2\alpha,0\right)$	—	—	—	12×1
	S_{31}	$\mathsf{Perm}\left(\alpha,\alpha,\alpha,1-3\alpha\right)$	—	—	4×1	4×1
	S_{22}	$\mathsf{Perm}\left(\alpha,\alpha,\frac{1}{2}-\alpha,\frac{1}{2}-\alpha\right)$	—	—	—	6×1
		# free parameters	—	—	2	4
		# nodes total	4	11	24	45
		cubature degree	1	3	5	7

$p=1$ $\qquad p=2$ $\qquad p=3$ $\qquad p=4$
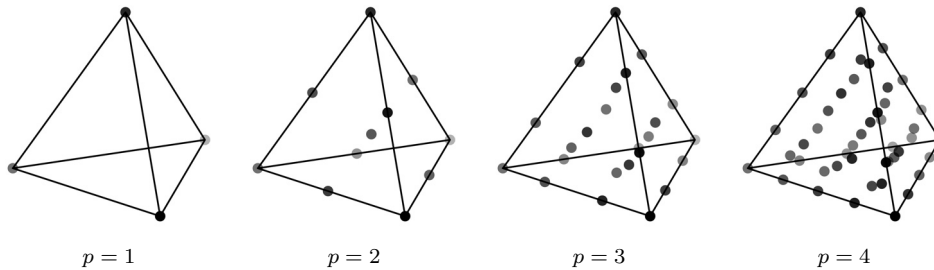
FIG. 2. *Node distributions for cubature rules adopted for the SBP operators on tetrahedra.*

Remark 4. The boundary operators, when restricted to the boundary nodes, are dense matrices. Contrast this with the tensor-product case, where the boundary operators are diagonal matrices. In the simplex case, we have not found a way to construct diagonal E_x, E_y, and E_z that are sufficiently accurate.

4.3. The antisymmetric part. The accuracy conditions are used to determine the antisymmetric matrices S_x, S_y, and S_z. We will describe the process for S_x, since it can be adapted in a straightforward way to S_y and, in the case of the tetrahedron, to S_z.

In theory, we can compute S_x using the monomials that appear in the SBP operator definition; however, the monomials are known to produce ill-conditioned Vandermonde matrices. Instead, we follow the standard practice in spectral-element methods and apply the accuracy conditions to appropriate orthogonal bases on the triangle and tetrahedron [22, 11, 16]. Unlike finite- and spectral-element methods, the basis alone does not completely specify an SBP operator.

Let P and P_x be the matrices whose columns are the orthogonal basis function values and derivatives, respectively, evaluated at the nodes. Then the accuracy con-

ditions imply $D_x P = P_x$, or, in terms of the unknown S_x,

$$S_x P = H P_x - \frac{1}{2} E_x P.$$

This can be recast as the linear system

(4.1) $$A q = b,$$

where q denotes a vector whose entries are the strictly lower part of S_x:

$$q \left(\tfrac{(i-2)(i-1)}{2} + j \right) = (S_x)_{i,j}, \qquad 2 \leq i \leq n, 1 \leq j < i.$$

There are $(n-1)n/2$ unknowns and $n \times \binom{p+d}{d}$ equations in (4.1); thus, for the operators considered here, there are more equations than unknowns. Fortunately, the compatibility conditions ensure that the system is consistent. Indeed, for $p \geq 3$ the rank of A is actually less than the size of q, so there are an infinite number of solutions. In these cases, we choose the minimum-norm least-squares solution [15] to (4.1).

4.4. Similarities and differences compared with existing operators. There is a vast literature on high-order discretizations for simplex elements, so we focus on the three that share the most in common with the proposed SBP operators: the diagonal mass matrix SE method [8, 29, 14], the SD method [25], and the nodal discontinuous Galerkin (NDG) method [16].

Our norm matrices H are identical to the lumped mass matrices in the SE method. The difference between the methods arises in the definition of Q_x. In the SE method of Giraldo and Taylor [14], the Q_x matrix is defined as

$$\left(Q_x^{\mathrm{SE}} \right)_{i,j} = \sum_{k=0}^{n} H_{k,k} \phi_i(x_k, y_k) \frac{\partial \phi_j}{\partial x}(x_k, y_k),$$

where $\{\phi_i\}_{i=1}^{n}$ is the so-called cardinal basis. For a degree p operator, the cardinal basis is a polynomial nodal basis that is a superset of the basis for degree p polynomials; the basis contains polynomials of degree greater than p, because the number of nodes n is greater than $\binom{p+d}{d}$ in general. Consequently, the cubature defined by H is not necessarily exact for the product $\phi_i \partial \phi_j / \partial x$ when $p \geq 2$, and the resulting Q_x^{SE} does not satisfy the SBP definition for the $p \geq 2$ discretizations. Indeed, as the results below demonstrate, the higher-order SE operators are unstable and require a skew-symmetric formulation, filtering, or numerical dissipation *even for linear problems.*

Remark 5. The Q_x^{SE} matrix in the diagonal mass matrix SE method can be made to satisfy the SBP definition by using a cubature rule that is exact for the cardinal basis; however, such a cubature rule would require additional cubature points and would defeat the purpose (i.e., efficiency) of collocating the cubature and basis nodes.

The SBP simplex operators can also be viewed as a special case of the SD method in which the unknowns and fluxes are collocated. As pointed out in [25], this means that our proposed SBP operators require more unknowns to achieve a given accuracy than SD methods; however, collocation eliminates the reconstruction step, so there is a tradeoff between memory and floating-point operations. In addition, the relative increase in unknowns is more pronounced for discontinuous discretizations, such as SD, than for continuous ones; if we assemble a global SBP operator, as described below, then the number of unknowns can be significantly reduced.

Finally, our diagonal-norm SBP operators also share much in common with the simplex-based NDG method; see, for example, the monograph [16]. Indeed, it is easy to show that the element-level simplex operators used in the NDG method are dense-norm SBP operators. Compared to diagonal-norm SBP operators, these nodal FE operators require fewer nodes for the same design accuracy; however, they are not attractive for C^0 solution spaces when explicit time marching is used, because they yield mass matrices that are nontrivial to invert.

4.5. Assembly of global SBP operators from elemental operators. The SBP operators defined in sections 4.1–4.3 can be used in an NDG formulation [16] with elements coupled weakly using, for example, SATs [12, 4]. An alternative use for these element-based operators, and the one pursued here, is to mimic the continuous Galerkin formulation. That is, we assemble global SBP operators from the elemental ones.

We need to introduce some additional notation to help describe the assembly process and facilitate the proof of Theorem 4.1 below. Suppose the domain Ω is partitioned into a set of L nonoverlapping subdomains $\Omega^{(l)}$ with boundaries $\Gamma^{(l)}$:

$$\Omega = \bigcup_{l=1}^{L} \bar{\Omega}^{(l)} \qquad \text{and} \qquad \Omega^{(k)} \cap \Omega^{(l)} = \emptyset \quad \forall\, k \neq l,$$

where $\bar{\Omega}^{(l)} = \Omega^{(l)} \cup \Gamma^{(l)}$ denotes the closure of $\Omega^{(l)}$.

Each subdomain is associated with a set of nodes $S^{(l)} \equiv \{(x_i^{(l)}, y_j^{(l)})\}_{i=1}^{n}$ such that $(x_i^{(l)}, y_i^{(l)}) \in \bar{\Omega}^{(l)}$. In the present context, some of the nodes in $S^{(l)}$ will lie on the boundary $\Gamma^{(l)}$ and be shared by adjacent subdomains.

Let $S \equiv \cup_l S^{(l)}$. Suppose there are $\tilde{n}$ unique nodes in S, and let each node be assigned a unique global index. Suppose $\tilde{\imath}$ is the global index corresponding to the ith local node of element l. We define $\mathsf{Z}^{(l)}(i, j)$ to be the $\tilde{n} \times \tilde{n}$ matrix with zeros everywhere except in the $(\tilde{\imath}, \tilde{\jmath})$ entry, which is unity. If $e_{\tilde{\imath}}$ denotes the $\tilde{\imath}$th column of the $\tilde{n} \times \tilde{n}$ identity, then $\mathsf{Z}^{(l)}(i, j) = e_{\tilde{\imath}} e_{\tilde{\jmath}}^{\mathrm{T}}$.

We can now state and prove the following result, which applies to both diagonal- and dense-norm SBP operators.

THEOREM 4.1. *Let* $\mathsf{D}_x^{(l)} = \left(\mathsf{H}^{(l)}\right)^{-1} \mathsf{Q}_x^{(l)}$ *be a degree p SBP operator for the first derivative $\partial/\partial x$ on the node set $S^{(l)}$. If*

$$\mathsf{H} \equiv \sum_{l=1}^{L} \sum_{i=1}^{n} \sum_{j=1}^{n} \mathsf{H}_{i,j}^{(l)} \mathsf{Z}^{(l)}(i, j),$$

$$\mathsf{Q}_x \equiv \sum_{l=1}^{L} \sum_{i=1}^{n} \sum_{j=1}^{n} \left(\mathsf{Q}_x^{(l)}\right)_{i,j} \mathsf{Z}^{(l)}(i, j),$$

then $\mathsf{D}_x = \mathsf{H}^{-1} \mathsf{Q}_x$ *is a degree p SBP operator on the global node set S.*

Proof. We need to check each of the three properties in Definition 2.1.

1. The first property is straightforward, albeit tedious, to verify. H^{-1} exists by

property 2, which is shown to hold independently below, so we have

$$
\mathsf{D}_x \boldsymbol{p}_k = \mathsf{H}^{-1}\mathsf{Q}_x \boldsymbol{p}_k = \mathsf{H}^{-1}\left[\sum_{l=1}^{L}\sum_{i=1}^{n}\sum_{j=1}^{n}\left(\mathsf{Q}_x^{(l)}\right)_{i,j}\mathsf{Z}^{(l)}(i,j)\right]\boldsymbol{p}_k
$$

$$
= \mathsf{H}^{-1}\sum_{l=1}^{L}\sum_{i=1}^{n}\sum_{j=1}^{n}\sum_{r=1}^{n}\mathsf{H}_{i,r}^{(l)}\left(\mathsf{D}_x^{(l)}\right)_{r,j}e_{\tilde{\imath}}\mathcal{P}_k(x_{\tilde{\jmath}},y_{\tilde{\jmath}})
$$

$$
= \mathsf{H}^{-1}\sum_{l=1}^{L}\sum_{i=1}^{n}\sum_{r=1}^{n}\mathsf{H}_{i,r}^{(l)}e_{\tilde{\imath}}\sum_{j=1}^{n}\left(\mathsf{D}_x^{(l)}\right)_{r,j}\mathcal{P}_k(x_j,y_j)
$$

$$
= \mathsf{H}^{-1}\sum_{l=1}^{L}\sum_{i=1}^{n}\sum_{r=1}^{n}\mathsf{H}_{i,r}^{(l)}e_{\tilde{\imath}}\frac{\partial\mathcal{P}_k}{\partial x}(x_r,y_r)
$$

$$
= \mathsf{H}^{-1}\left[\sum_{l=1}^{L}\sum_{i=1}^{n}\sum_{r=1}^{n}\mathsf{H}_{i,r}^{(l)}\mathsf{Z}^{(l)}(i,r)\right]\boldsymbol{p}_k'.
$$

But the term in brackets above is the definition of H, so we are left with $\mathsf{D}_x\boldsymbol{p}_k = \boldsymbol{p}_k'$, as desired.

2. H is clearly symmetric by construction. To show that it is positive definite, let $\boldsymbol{u}\in\mathbb{R}^{\tilde{n}}$ be a nonzero vector and consider

$$
\boldsymbol{u}^{\mathrm{T}}\mathsf{H}\boldsymbol{u} = \boldsymbol{u}^{\mathrm{T}}\left[\sum_{l=1}^{L}\sum_{i=1}^{n}\sum_{j=1}^{n}\mathsf{H}_{i,j}^{(l)}\mathsf{Z}^{(l)}(i,j)\right]\boldsymbol{u} = \sum_{l=1}^{L}\left[\sum_{i=1}^{n}\sum_{j=1}^{n}u_i\mathsf{H}_{i,j}^{(l)}u_j\right]\geq 0,
$$

where the inequality follows since each $\mathsf{H}^{(l)}$ is positive definite; however, we cannot have $\boldsymbol{u}^{\mathrm{T}}\mathsf{H}\boldsymbol{u} = 0$, since this would imply that all the subvectors $\mathsf{Z}^{(l)}(i,j)u_j$ are zero and, consequently, that $\boldsymbol{u} = \boldsymbol{0}$. Therefore H is positive definite.

3. Finally, we form the decomposition $\mathsf{Q}_x = \mathsf{S}_x + \frac{1}{2}\mathsf{E}_x$, where

$$
\mathsf{S}_x = \sum_{l=1}^{L}\sum_{i=1}^{n}\sum_{j=1}^{n}(\mathsf{S}_x)^{(l)}(i,j)\mathsf{Z}_{i,j}^{(l)},
$$

$$
\mathsf{E}_x = \sum_{l=1}^{L}\sum_{i=1}^{n}\sum_{j=1}^{n}\mathsf{E}_x^{(l)}(i,j)\mathsf{Z}_{i,j}^{(l)}.
$$

The matrix S_x is antisymmetric because it is the sum of antisymmetric matrices. Similarly, E_x is symmetric because it is the sum of symmetric matrices. In addition,

$$
\boldsymbol{p}_k^{\mathrm{T}}\mathsf{E}_x\boldsymbol{p}_m = \sum_{l=1}^{L}\sum_{i=1}^{n}\sum_{j=1}^{n}\mathsf{E}_x^{(l)}(i,j)\boldsymbol{p}_k^{\mathrm{T}}\mathsf{Z}_{i,j}^{(l)}\boldsymbol{p}_m
$$

$$
= \sum_{l=1}^{L}\oint_{\Gamma^{(l)}}\mathcal{P}_k\mathcal{P}_m n_x\mathrm{d}\Gamma
$$

$$
= \oint_{\Gamma}\mathcal{P}_k\mathcal{P}_m n_x\mathrm{d}\Gamma,
$$

where we have used the fact that the boundary fluxes of adjacent elements cancel analytically. Thus, property 3 is satisfied. □

5. Verification studies. The two-dimensional linear advection equation is used to verify and study the triangular-element SBP operators of section 4. In particular, we consider the problem

$$\frac{\partial \mathcal{U}}{\partial t} + \frac{\partial \mathcal{U}}{\partial x} + \frac{\partial \mathcal{U}}{\partial y} = 0 \qquad \forall\, (x, y) \in \Omega = [0, 1]^2,$$

$$\mathcal{U}(x, 0, t) = \mathcal{U}(x, 1, t) \qquad \text{and} \qquad \mathcal{U}(0, y, t) = \mathcal{U}(1, y, t),$$

$$\mathcal{U}(x, y, 0) = \begin{cases} 1 - (4r^2 - 1)^5 & \text{if } r \le \frac{1}{2}, \\ 1 & \text{otherwise,} \end{cases}$$

where $r(x, y) \equiv \sqrt{(x - \frac{1}{2})^2 + (y - \frac{1}{2})^2}$. The boundary conditions imply periodicity in both the x and y directions, and the PDE implies an advection velocity of $(1, 1)$. The initial condition is a C^4 continuous bump function that is periodic on Ω.

A nonuniform mesh for the square domain Ω is generated in order to eliminate possible error cancellations that may arise on uniform grids. The vertices of the mesh are given by

$$x_{i,j} = \frac{i}{N} + \frac{1}{40} \sin\left(\frac{2\pi i}{N}\right) \sin\left(\frac{2\pi j}{N}\right), \qquad y_{i,j} = \frac{j}{N} + \frac{1}{40} \sin\left(\frac{2\pi i}{N}\right) \sin\left(\frac{2\pi j}{N}\right),$$

where N is the number of elements along an edge of Ω and $i, j = 0, 1, 2, \ldots, N$. The nominal element size is $h \equiv 1/N$. A triangular mesh is generated by dividing each quadrilateral $\{x_{i,j}, x_{i+1,j}, x_{i,j+1}, x_{i+1,j+1}\}$ along the diagonal from $x_{i+1,j}$ to $x_{i,j+1}$. Finally, for an SBP element of degree p, the reference-element nodes are mapped (affinely) to each triangle in the mesh. Figure 3 illustrates a representative mesh for $p = 3$ and $N = 12$.
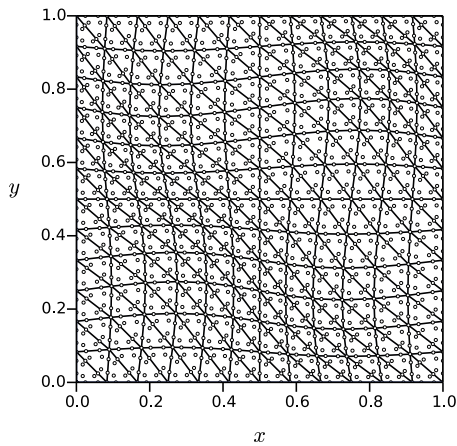

FIG. 3. *Example mesh with $p = 3$ and $N = 12$ for accuracy and energy-norm studies.*
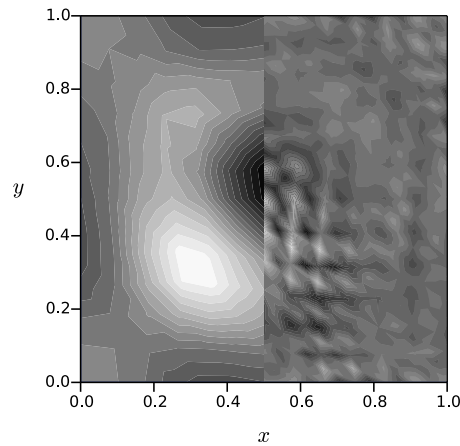

FIG. 4. *Solution error after one period, $t = T$, for the $p = 1$ (left) and $p = 2$ (right) C-SBP discretizations with $N = 12$.*

Maximally stable CFL numbers for the SBP operators on the nonuniform mesh with $N = 32$.

	$p = 1$	$p = 2$	$p = 3$	$p = 4$
C-SBP $\text{CFL}_{\max}$	1.885	2.257	1.816	1.570
D-SBP $\text{CFL}_{\max}$	0.696	1.269	1.157	1.148

Remark 6. The use of an affine mapping on each element ensures that the mapping Jacobian is elementwise constant; consequently, the transformed PDE has constant coefficients in the reference space and the FD operator remains SBP. More generally, curvilinear elements would require constructing SBP operators for each curved element.

We consider both continuous (C-SBP) and discontinuous (D-SBP) discretizations using the SBP operators. The global operators for the C-SBP discretizations are constructed using the assembly process described in section 4.5. In addition, the periodic boundaries are transparent to the global C-SBP operators; that is, nodes that coincide on the periodic boundary are considered the same. The D-SBP discretization of the surface fluxes follows the NDG method outlined, for example, in Hesthaven and Warburton [16, Chapter 6]. We use SATs with a penalty parameter of $\sigma = 1$, which is equivalent to the use of upwind numerical flux functions.

The classical fourth-order Runge–Kutta scheme is used to discretize the time derivative, and the initial condition is sampled at the nodes. The maximally stable CFL number for each SBP operator was identified for $N = 32$ using golden section optimization, where the CFL number was defined as $\sqrt{2}\Delta t/(h\Delta r) = \sqrt{2}N\Delta t/\Delta r$ for a time-step size of Δt and an advection velocity of $(1, 1)$; the nominal node spacing is $h\Delta r$, where $h = 1/N$ and Δr denotes the minimum distance between cubature nodes on a right triangle with vertices at $(0,0)$, $(1,0)$, and $(0,1)$. Each discretization was run for five periods, $t \equiv 5T = 5$ units, and was considered stable if the final solution norm was less than or equal to the initial solution norm. The results of the optimization are listed in Table 3.

5.1. Accuracy and efficiency studies. Figures 5 and 6 plot the normalized H-norm error for the C-SBP and D-SBP discretizations, respectively, for SBP operator degrees 1–4 and a range of N. Specifically, if $\boldsymbol{u}_0$ is the initial solution and $\boldsymbol{u}$ is the solution at $t = T$, then the error is

$$\text{H-norm Error} \equiv \sqrt{(\boldsymbol{u} - \boldsymbol{u}_0)^{\text{T}} \, \text{H} \, (\boldsymbol{u} - \boldsymbol{u}_0)},$$

where H is the appropriate SBP norm for the scheme. The error is normalized by the H-norm of the initial condition. The mesh resolution ranges from $N = 4$ to $N = 64$ in increments of 4. Each case was time marched using a CFL number of $0.9\text{CFL}_{\max}$, which was sufficiently small to produce negligible temporal discretization errors.

Remark 7. Recall that $\text{H}_{i,i}$ are weights for a cubature rule of degree $2p-1$, so the error computed using the H-norm approximates the integral L^2 error. The H-norm error is commonly used in the SBP literature. Alternatively, one could choose a basis that interpolates the error at the nodes, e.g., the cardinal basis used in [14], and then compute the L^2 error using a sufficiently accurate cubature rule; however, the choice of basis is not unique for FD operators, and it is not clear how to select one basis over another in this context.
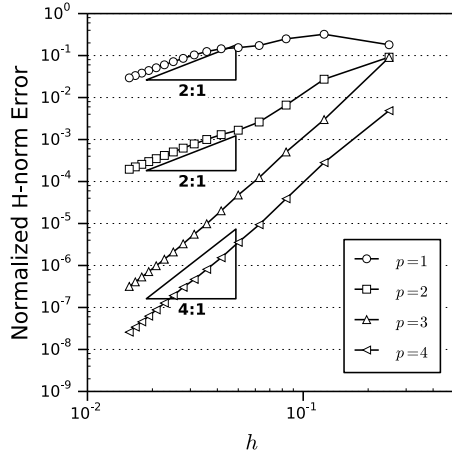
FIG. 5. H-*norm error between the C-SBP solution after five periods, $t = 5T$, and the initial condition for different mesh spacing and operators.*
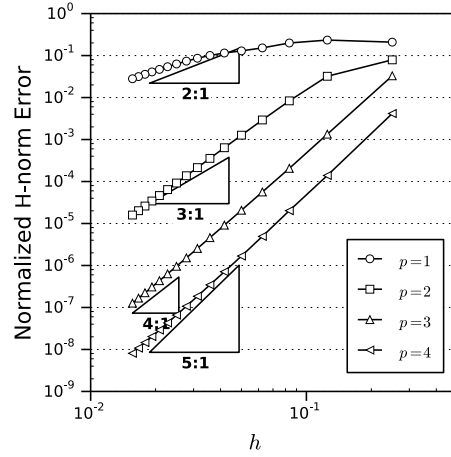
FIG. 6. H-*norm error between the D-SBP solution after five periods, $t = 5T$, and the initial condition for different mesh spacing and operators.*

The results in Figure 6 indicate that the D-SBP discretizations and the odd-order C-SBP discretizations exhibit asymptotic convergence rates of $O(h^{p+1})$. In contrast, the C-SBP discretizations based on the $p = 2$ and $p = 4$ operators have convergence rates of $O(h^p)$. These discretizations experience even-odd decoupling, i.e., checkerboarding, which is illustrated in Figure 4 by comparing the spatial error at $t = T$ for the $p = 1$ and $p = 2$ C-SBP discretizations; the $p = 1$ error is smooth, whereas the $p = 2$ error is oscillatory. Checkerboarding is not unique to the SBP simplex operators and can be observed with one-dimensional SBP operators as well as FEMs. We are currently investigating methods to address this issue with the even-order C-SBP discretizations.

Remark 8. The optimal convergence rates produced by the D-SBP scheme are a consequence of the dissipation introduced by the upwind SATs; see Figure 9 for the eigenvalue spectra of the schemes. We have verified that using symmetric SATs leads to pure imaginary eigenvalues and suboptimal convergence rates.

Figures 7 and 8 plot the normalized H-norm error versus CPU time for both the C-SBP and D-SBP discretizations. The runs were performed on an Intel Core i5-3570K processor, and the code was implemented in Julia version 0.4.0. The efficiency provided by the high-order operators is apparent in both the continuous and discontinuous cases.

5.2. Stability studies. Figure 9 shows the spectra of the C-SBP, D-SBP, and SE spatial discretizations for the linear advection problem. Specifically, these eigenvalues are for the spatial operators scaled by $\Delta r/(N\sqrt{2})$, where $N = 12$. This scaling, which is consistent with the CFL number definition, allows a qualitative comparison of the maximum allowable time steps.

The eigenvalues of the C-SBP operators are imaginary to machine precision, which mimics the continuous spectrum for this periodic problem. This is expected, because the boundary operators $\mathsf{E}_x^{(l)}$ and $\mathsf{E}_y^{(l)}$ cancel between adjacent elements when the SBP derivative operator is assembled, leaving only the antisymmetric parts. The eigenvalues of the D-SBP operators have nonpositive real parts to machine precision;
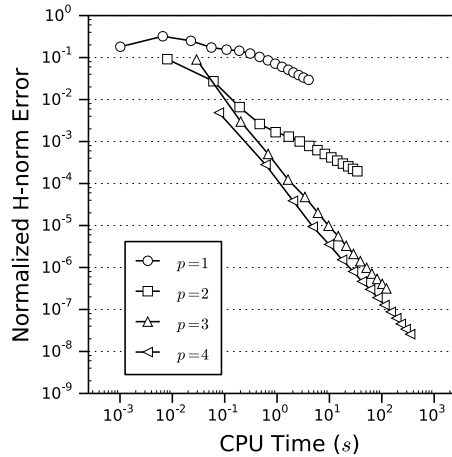
FIG. 7. *Normalized* H*-norm error of the C-SBP solutions after one period versus CPU time measured in seconds.*
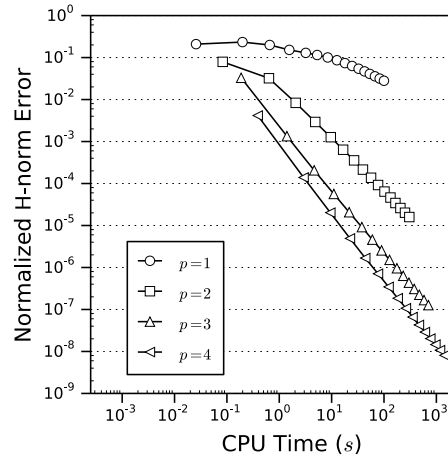
FIG. 8. *Normalized* H*-norm error of the D-SBP solutions after one period versus CPU time measured in seconds.*

this is also expected, since the SATs introduce dissipation. Finally, the SE operator for $p = 1$ also has a purely imaginary spectrum, because it is identical to the linear SBP operator; however, the spectra of the high-order SE operators have a positive real component.

The consequences of the eigenvalue distributions are evident when the linear advection problem is integrated for five periods. Figure 10 plots the difference between the solution H-norm at time $t \in [0, 5]$ and the initial solution norm, i.e., the change in "energy,"

$$\Delta E = \boldsymbol{u}_n^{\mathrm{T}} \mathsf{H} \boldsymbol{u}_n - \boldsymbol{u}_0^{\mathrm{T}} \mathsf{H} \boldsymbol{u}_0,$$

where $\boldsymbol{u}_n$ denotes the discrete solution at time step n. For this study, $N = 12$ and the CFL number was fixed at 0.01 to reduce temporal errors.

The energy history in Figure 10 clearly shows that the SE operators are unstable for this linear advection problem, while the SBP operators are stable. The small change in the C-SBP energy is due to round-off and temporal errors; the latter can be reduced by using a different time-marching method, e.g., leapfrog, or at the cost of using a sufficiently small CFL number.

6. Conclusions and discussion. We proposed a definition for multidimensional SBP operators that is a natural extension of one-dimensional SBP definitions. We studied the theoretical implications of the definition in the case of diagonal-norm operators, and showed that the multidimensional operators retain the attractive properties of tensor-product SBP operators. A significant theoretical result of this work is that a diagonal-norm SBP operator of degree p exists for a given domain if and only if there exists a cubature rule of degree $2p - 1$ with positive weights and an associated full-rank Vandermonde matrix, i.e., the $n \times n_p^*$ matrix of a polynomial basis evaluated at the cubature nodes is full column rank. We showed that an SBP-SAT discretization of the linear advection equation is time stable.

We presented a novel—at least for SBP operators—assembly procedure that constructs SBP operators for a global domain from elementwise SBP operators. The procedure offers an alternative to using interface SATs and can result in SBP discretizations with significantly fewer degrees of freedom.
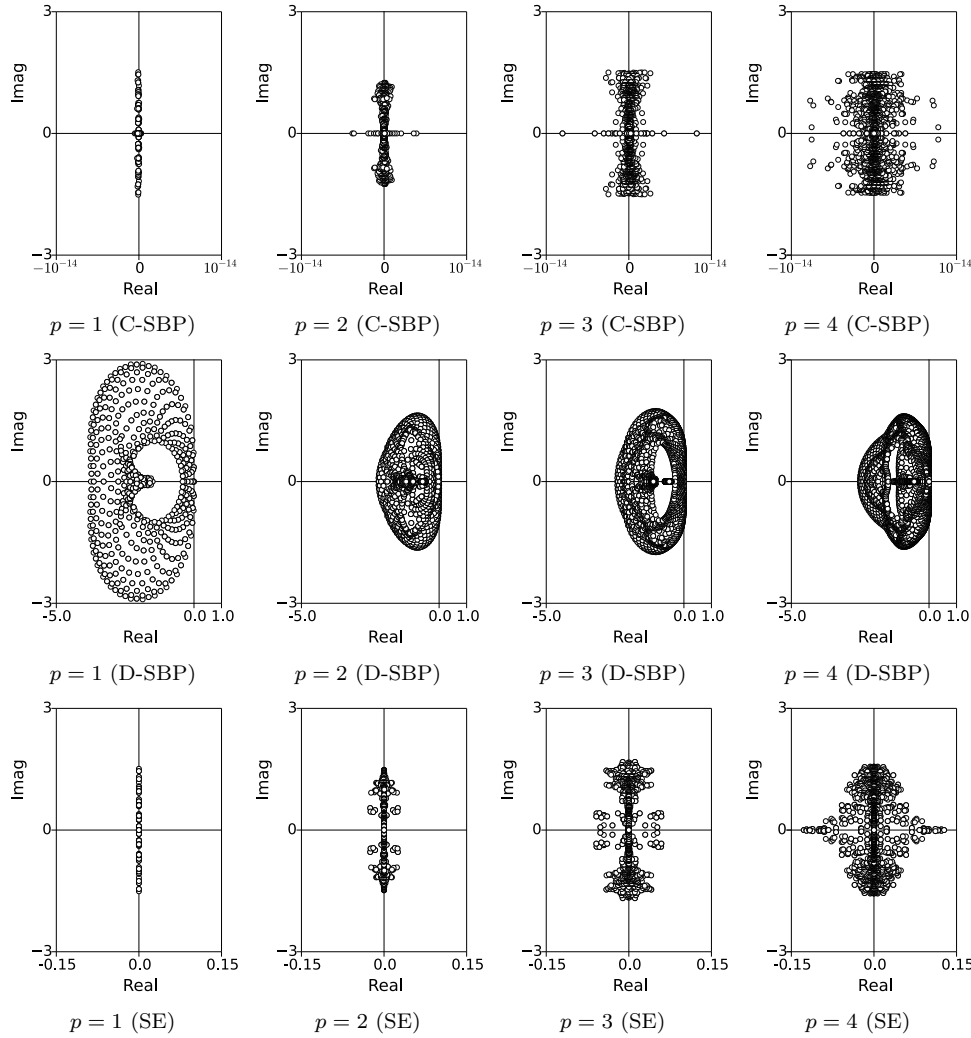
FIG. 9. *Eigenvalue distributions for the C-SBP (upper row), the D-SBP (middle row), and the SE (lower row) spatial discretizations of the linear advection problem. Note the different ranges for the real axes.*

The multidimensional SBP definition and theory were illustrated by constructing diagonal-norm SBP operators for the triangle and tetrahedron. To the best of our knowledge, this is the first example of diagonal-norm SBP operators of degree $p \geq 2$ on these domains. We verified the triangle-element SBP operators using both continuous and discontinuous (i.e., SAT) interelement coupling. Results for linear advection on a doubly periodic domain demonstrated the time stability and accuracy of the SBP discretizations. The results suggest that the proposed operators could be effective for the long-time simulation of turbulent flows on complex domains.

We believe that the above simplex operators are useful, but they do not fully demonstrate the potential value of multidimensional SBP operators. The flexibility offered by the SBP definition can be used to achieve various objectives; we list three below.
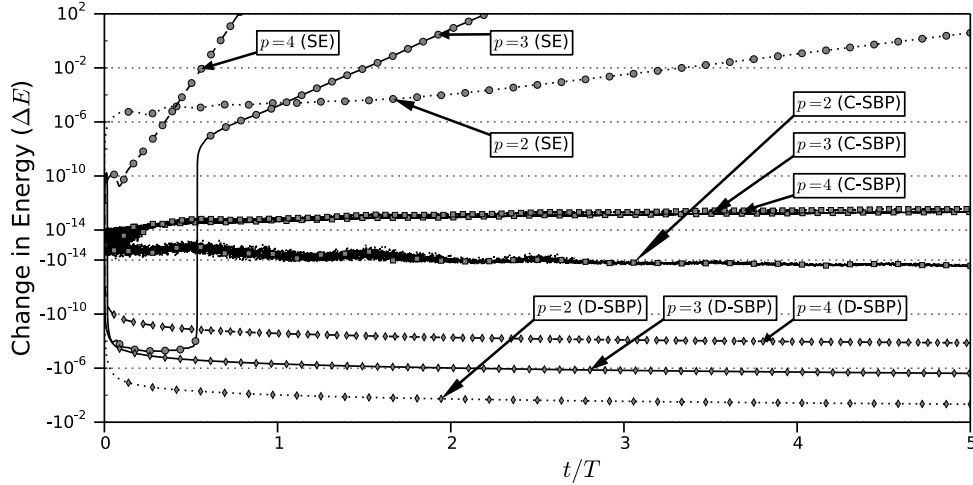
FIG. 10. *Time history of the change in the solution energy norm. Note the use of a symmetric logarithmic scale on the vertical axis.*

- SBP operators can be constructed on simplices with uniform node distributions, which will facilitate multigrid on unstructured grids. Uniform nodes also make adjoint-based error estimation easier and cheaper, since high-order operators can be applied on the same nodes, making it unnecessary to solve the adjoint on a finer grid [17].
- It is possible to reduce time-step restrictions and improve operator conditioning. For example, the simplex operators presented in this work have smaller time-step restrictions than the SE method when the latter is stabilized using the skew-symmetric form.
- By increasing the number of nodes in a given element, sparse multidimensional SBP operators can be constructed.

We acknowledge that building operators that meet the above objectives is not straightforward and is the goal of future research.

Appendix A. Decomposition of the SAT matrix $\beta_x \mathsf{E}_x + \beta_y \mathsf{E}_y$. Let $\mathsf{E} \equiv \beta_x \mathsf{E}_x + \beta_y \mathsf{E}_y$. Recall the block-matrix definition of E_x used in the proof of Theorem 3.3. Using that definition and a similar definition for E_y, we have

$$\tilde{\mathsf{V}}^{-\mathrm{T}} \mathsf{E} \tilde{\mathsf{V}}^{-1} = \tilde{\mathsf{V}}^{-\mathrm{T}} \begin{bmatrix} \tilde{\mathsf{E}} & \mathsf{F}^T \\ \mathsf{F} & \mathsf{G} \end{bmatrix} \tilde{\mathsf{V}}^{-1} \equiv \beta_x \tilde{\mathsf{V}}^{-\mathrm{T}} \begin{bmatrix} \tilde{\mathsf{E}}_x & \mathsf{F}_x^{\mathrm{T}} \\ \mathsf{F}_x & \mathsf{G}_x \end{bmatrix} \tilde{\mathsf{V}}^{-1} + \beta_y \tilde{\mathsf{V}}^{-\mathrm{T}} \begin{bmatrix} \tilde{\mathsf{E}}_y & \mathsf{F}_y^{\mathrm{T}} \\ \mathsf{F}_y & \mathsf{G}_y \end{bmatrix} \tilde{\mathsf{V}}^{-1}.$$

From the definitions of $\tilde{\mathsf{E}}_x$ and $\tilde{\mathsf{E}}_y$, we have that the entries in the block $\tilde{\mathsf{E}}$ are given by

$$\left(\tilde{\mathsf{E}} \right)_{k,m} = \oint_{\Gamma} \mathcal{P}_k(x,y) \mathcal{P}_m(x,y) \left(\beta_x n_x + \beta_y n_y \right) \mathrm{d}\Gamma \qquad \forall\, k, m \in \{1, \ldots, n_\tau^*\},$$

where $\mathcal{P}_k$ and $\mathcal{P}_l$ have total degrees less than or equal to τ. We can decompose $\tilde{\mathsf{E}}$ by breaking the above integral into two integrals, one over Γ_+ and one over Γ_-:

$$\left(\tilde{\mathsf{E}} \right)_{k,m} = \oint_{\Gamma_+} \mathcal{P}_k \mathcal{P}_m \left(\beta_x n_x + \beta_y n_y \right) \mathrm{d}\Gamma + \oint_{\Gamma_-} \mathcal{P}_k \mathcal{P}_m \left(\beta_x n_x + \beta_y n_y \right) \mathrm{d}\Gamma = \tilde{\mathsf{E}}_+ + \tilde{\mathsf{E}}_-$$

$$\forall\, k, m \in \{1, \ldots, n_\tau^*\},$$

where $\tilde{\mathsf{E}}_+$ and $\tilde{\mathsf{E}}_-$ are equated with the integrals over Γ_+ and Γ_-, respectively.

LEMMA A.1. *The matrix $\tilde{\mathsf{E}}_-$ is negative semidefinite, and the matrix $\tilde{\mathsf{E}}_+$ is positive semidefinite.*

Proof. We prove the result for $\tilde{\mathsf{E}}_-$, since the proof for the positive definite matrix is analogous. Let $\boldsymbol{u} \in \mathbb{R}^{n_p^*}$ be an arbitrary nonzero vector, and let u_k denote its entries. Then

$$\boldsymbol{u}^T \tilde{\mathsf{E}}_- \boldsymbol{u} = \sum_{k=1}^{n_\tau^*} \sum_{l=1}^{n_\tau^*} \oint_{\Gamma_-} (u_k \mathcal{P}_k(x,y)) (u_l \mathcal{P}_l(x,y)) (\beta_x n_x + \beta_y n_y) \, \mathrm{d}\Gamma$$

$$= \oint_{\Gamma_-} [\mathcal{U}(x,y)]^2 (\beta_x n_x + \beta_y n_y) \, \mathrm{d}\Gamma,$$

where $\mathcal{U}(x,y) \equiv \sum_{k=1}^{n_\tau^*} u_k \mathcal{P}_k(x,y)$. The integrand in the above is the product of a squared polynomial function and the nonpositive quantity $(\beta_x n_x + \beta_y n_y) \le 0$ for all $(x,y) \in \Gamma_-$. Thus the desired result follows.   □

We now turn to the main result of this appendix.

THEOREM A.2. *Suppose $\mathsf{F}_x = 0$ and $\mathsf{F}_y = 0$ in the definitions of E_x and E_y. Then, for any $\beta_x, \beta_y \in \mathbb{R}$, the matrix $\mathsf{E} \equiv \beta_x \mathsf{E}_x + \beta_y \mathsf{E}_y$ can be decomposed into $\mathsf{E} = \mathsf{E}_+ + \mathsf{E}_-$, where E_+ is positive semidefinite, E_- is negative semidefinite, and $\mathsf{E}_\pm$ satisfy the accuracy conditions*

$$(A.1) \qquad \boldsymbol{p}_k^{\mathrm{T}} \mathsf{E}_\pm \boldsymbol{p}_m = \oint_{\Gamma_\pm} \mathcal{P}_k \mathcal{P}_m (\beta_x n_x + \beta_y n_y) \, \mathrm{d}\Gamma \qquad \forall \, k, m \in \{1, 2, \ldots, n_\tau^*\}.$$

Proof. Consider the decomposition

$$\mathsf{E} = \mathsf{E}_+ + \mathsf{E}_- = \tilde{\mathsf{V}}^{-\mathrm{T}} \begin{bmatrix} \tilde{\mathsf{E}}_+ & (\mathsf{F}_+)^{\mathrm{T}} \\ \mathsf{F}_+ & \mathsf{G}_+ \end{bmatrix} \tilde{\mathsf{V}}^{-1} + \tilde{\mathsf{V}}^{-\mathrm{T}} \begin{bmatrix} \tilde{\mathsf{E}}_- & (\mathsf{F}_-)^{\mathrm{T}} \\ \mathsf{F}_- & \mathsf{G}_-, \end{bmatrix} \tilde{\mathsf{V}}^{-1},$$

where $\tilde{\mathsf{E}}_\pm$ are defined above and the pairs $(\mathsf{F}_+, \mathsf{F}_-)$ and $(\mathsf{G}_+, \mathsf{G}_-)$ are yet-to-be-determined decompositions of $\beta_x \mathsf{F}_x + \beta_y \mathsf{F}_y$ and $\beta_x \mathsf{G}_x + \beta_y \mathsf{G}_y$, respectively; note that the above decomposition of E is distinct from its definition, which involves E_x and E_y.

The accuracy of the matrices E_+ and E_-, as defined above, can be established using the same approach used in the proof of Theorem 3.3. Therefore, we focus on showing that E_- can be made negative semidefinite; again, an analogous proof can be used to show E_+ is positive semidefinite.

To prove that E_- is negative semidefinite, it suffices to show that the matrix

$$\begin{bmatrix} \tilde{\mathsf{E}}_- & (\mathsf{F}_-)^{\mathrm{T}} \\ \mathsf{F}_- & \mathsf{G}_- \end{bmatrix}$$

is negative semidefinite. This will be the case if we can ensure G_- is negative definite and the corresponding Schur complement,

$$\mathsf{S}_- \equiv \tilde{\mathsf{E}}_- - (\mathsf{F}_-)^{\mathrm{T}} (\mathsf{G}_-)^{-1} \mathsf{F}_-,$$

is negative semidefinite; see, for example, [2, Appendix A.5.5].

We first tackle the definiteness of G_-. Recall that G_x and G_y are symmetric but otherwise arbitrary. Therefore, the matrix $\mathsf{G} = \beta_x \mathsf{G}_x + \beta_y \mathsf{G}_y$ has the eigendecomposition $\mathsf{G} = \mathsf{R} \Lambda \mathsf{R}^{\mathrm{T}}$, where R holds the eigenvectors and the diagonal matrix Λ holds the

eigenvalues. For any set of eigenvalues, we can construct the nonunique decomposition

$$\mathsf{G} = \mathsf{R}\Lambda_+\mathsf{R}^{\mathrm{T}} + \mathsf{R}\Lambda_-\mathsf{R}^{\mathrm{T}}$$

such that Λ_+ is diagonal positive definite and Λ_- is diagonal negative definite; note that any zero eigenvalue in Λ can be decomposed as $c - c$ for arbitrary $c > 0$. Equating G_- with $\mathsf{R}\Lambda_-\mathsf{R}^{\mathrm{T}}$, we have that G_- is symmetric negative definite and therefore invertible.

Finally, we need to show that S_- is negative semidefinite. From Lemma A.1, we have that $\check{\mathsf{E}}_-$ is negative semidefinite. Thus, showing $\mathsf{S}_- \preceq 0$ is equivalent to showing[4]

$$\tilde{\mathsf{E}}_- \preceq \left(\mathsf{F}_-\right)^{\mathrm{T}}\left(\mathsf{G}_-\right)^{-1}\mathsf{F}_-.$$

This statement is true, provided that the entries in F_- are sufficiently small, which is certainly the case under the assumption that $\mathsf{F}_x = \mathsf{F}_y = 0$. This concludes the proof. □

Remark 9. In general, the assumption that $\mathsf{F}_x = \mathsf{F}_y = 0$ is stronger than necessary, since only $\mathsf{S}_- \preceq 0$ is required; however, it is not clear how to weaken this assumption when β_x and β_y are not known a priori.

Remark 10. The matrices E_x and E_y constructed for the simplex operators satisfy the conditions of Theorem A.2, i.e., $\mathsf{F}_x = \mathsf{F}_y = 0$.

Acknowledgment. All figures were produced using Matplotlib [20].

REFERENCES

[1] L. P. Bos, *On certain configurations of points in R^n which are unisolvent for polynomial interpolation*, J. Approx. Theory, 64 (1991), pp. 271–280, doi:10.1016/0021-9045(91)90063-G.
[2] S. Boyd and L. Vandenberghe, *Convex Optimization*, Cambridge University Press, Cambridge, UK, 2004.
[3] M. H. Carpenter and D. Gottlieb, *Spectral methods on arbitrary grids*, J. Comput. Phys., 129 (1996), pp. 74–86, doi:10.1006/jcph.1996.0234.
[4] M. H. Carpenter, D. Gottlieb, and S. Abarbanel, *Time-stable boundary conditions for finite-difference schemes solving hyperbolic systems: Methodology and application to high-order compact schemes*, J. Comput. Phys., 111 (1994), pp. 220–236, doi:10.1006/jcph.1994.1057.
[5] M. H. Carpenter, J. Nordström, and D. Gottlieb, *A stable and conservative interface treatment of arbitrary spatial accuracy*, J. Comput. Phys., 148 (1999), pp. 341–365, doi:10.1006/jcph.1998.6114.
[6] E. K.-Y. Chiu, Q. Wang, R. Hu, and A. Jameson, *A conservative mesh-free scheme and generalized framework for conservation laws*, SIAM J. Sci. Comput., 34 (2012), pp. A2896–A2916, doi:10.1137/110842740.
[7] E. K.-Y. Chiu, Q. Wang, and A. Jameson, *A conservative meshless scheme: General order formulation and application to Euler equations*, in 49th AIAA Aerospace Sciences Meeting, Orlando, FL, 2011, AIAA–2011–651, doi:10.2514/6.2011-651.
[8] G. Cohen, P. Joly, J. E. Roberts, and N. Tordjman, *Higher order triangular finite elements with mass lumping for the wave equation*, SIAM J. Numer. Anal., 38 (2001), pp. 2047–2078, doi:10.1137/S0036142997329554.
[9] D. C. Del Rey Fernández, *Generalized Summation-by-Parts Operators for First and Second Derivatives*, Ph.D. thesis, University of Toronto, Toronto, ON, Canada, 2015.
[10] D. C. Del Rey Fernández, P. D. Boom, and D. W. Zingg, *A generalized framework for nodal first derivative summation-by-parts operators*, J. Comput. Phys., 266 (2014), pp. 214–239, doi:10.1016/j.jcp.2014.01.038.
[11] M. Dubiner, *Spectral methods on triangles and other domains*, J. Sci. Comput., 6 (1991), pp. 345–390, doi:10.1007/BF01060030.

[4]The notation $A \preceq B$ means $A - B$ is negative semidefinite.

[12] D. FUNARO AND D. GOTTLIEB, *A new method of imposing boundary conditions in pseudospectral approximations of hyperbolic equations*, Math. Comp., 51 (1988), pp. 599–613.

[13] G. J. GASSNER, *A skew-symmetric discontinuous Galerkin spectral element discretization and its relation to SBP-SAT finite difference methods*, SIAM J. Sci. Comput., 35 (2013), pp. A1233–A1253, doi:10.1137/120890144.

[14] F. X. GIRALDO AND M. A. TAYLOR, *A diagonal-mass-matrix triangular-spectral-element method based on cubature points*, J. Engrg. Math., 56 (2006), pp. 307–322, doi:10.1007/s10665-006-9085-7.

[15] G. H. GOLUB AND C. F. VAN LOAN, *Matrix Computations*, 3rd ed., The Johns Hopkins University Press, Baltimore, MD, 1996.

[16] J. S. HESTHAVEN AND T. WARBURTON, *Nodal Discontinuous Galerkin Methods: Algorithms, Analysis, and Applications*, Springer-Verlag, New York, 2008.

[17] J. E. HICKEN, *Output error estimation for summation-by-parts finite-difference schemes*, J. Comput. Phys., 231 (2012), pp. 3828–3848, doi:10.1016/j.jcp.2012.01.031.

[18] J. E. HICKEN AND D. W. ZINGG, *A parallel Newton-Krylov solver for the Euler equations discretized using simultaneous approximation terms*, AIAA J., 46 (2008), pp. 2773–2786, doi:10.2514/1.34810.

[19] J. E. HICKEN AND D. W. ZINGG, *Summation-by-parts operators and high-order quadrature*, J. Comput. Appl. Math., 237 (2013), pp. 111–125, doi:10.1016/j.cam.2012.07.015.

[20] J. D. HUNTER, *Matplotlib: A 2D graphics environment*, Comput. Sci. Eng., 9 (2007), pp. 90–95, doi:10.1109/MCSE.2007.55.

[21] A. KITSON, R. I. MCLACHLAN, AND N. ROBIDOUX, *Skew-adjoint finite difference methods on nonuniform grids*, New Zealand J. Math., 32 (2003), pp. 139–159.

[22] T. KOORNWINDER, *Two-variable analogues of the classical orthogonal polynomials*, in Theory and Application of Special Functions, Academic Press, New York, 1975, pp. 435–495.

[23] H.-O. KREISS AND G. SCHERER, *Finite element and finite difference methods for hyperbolic partial differential equations*, in Mathematical Aspects of Finite Elements in Partial Differential Equations, Academic Press, New York, London, 1974, pp. 195–212.

[24] Y. LIU AND M. VINOKUR, *Exact integrations of polynomials and symmetric quadrature formulas over arbitrary polyhedral grids*, J. Comput. Phys., 140 (1998), pp. 122–147, doi:10.1006/jcph.1998.5884.

[25] Y. LIU, M. VINOKUR, AND Z. J. WANG, *Spectral difference method for unstructured grids. I. Basic formulation*, J. Comput. Phys., 216 (2006), pp. 780–801, doi:10.1016/j.jcp.2006.01.024.

[26] K. MATTSSON, *Summation by parts operators for finite difference approximations of second-derivatives with variable coefficients*, J. Sci. Comput., 51 (2012), pp. 650–682, doi:10.1007/s10915-011-9525-z.

[27] K. MATTSSON AND J. NORDSTRÖM, *Summation by parts operators for finite difference approximations of second derivatives*, J. Comput. Phys., 199 (2004), pp. 503–540, doi:10.1016/j.jcp.2004.03.001.

[28] Y. MORINISHI, T. S. LUND, O. V. VASILYEV, AND P. MOIN, *Fully conservative higher order finite difference schemes for incompressible flow*, J. Comput. Phys., 143 (1998), pp. 90–124, doi:10.1006/jcph.1998.5962.

[29] W. A. MULDER, *Higher-order mass-lumped finite elements for the wave equation*, J. Comput. Acoust., 9 (2001), pp. 671–680, doi:10.1142/S0218396X0100067X.

[30] J. NORDSTRÖM, *Conservative finite difference formulations, variable coefficients, energy estimates and artificial dissipation*, J. Sci. Comput., 29 (2006), pp. 375–404, doi:10.1007/s10915-005-9013-4.

[31] J. NORDSTRÖM, K. FORSBERG, C. ADAMSSON, AND P. ELIASSON, *Finite volume methods, unstructured meshes and strict stability for hyperbolic problems*, Appl. Numer. Math., 45 (2003), pp. 453–473, doi:10.1016/S0168-9274(02)00239-8.

[32] J. NORDSTRÖM, J. GONG, E. VAN DER WEIDE, AND M. SVÄRD, *A stable and conservative high order multi-block method for the compressible Navier-Stokes equations*, J. Comput. Phys., 228 (2009), pp. 9020–9035, doi:10.1016/j.jcp.2009.09.005.

[33] B. STRAND, *Summation by parts for finite difference approximations for d/dx*, J. Comput. Phys., 110 (1994), pp. 47–67, doi:10.1006/jcph.1994.1005.

[34] M. SVÄRD, *On coordinate transformations for summation-by-parts operators*, J. Sci. Comput., 20 (2004), pp. 29–42, doi:10.1023/A:1025881528802.

[35] M. SVÄRD, K. MATTSSON, AND J. NORDSTRÖM, *Steady-state computations using summation-by-parts operators*, J. Sci. Comput., 24 (2005), pp. 79–95, doi:10.1007/s10915-004-4788-2.

[36] F. D. WITHERDEN AND P. E. VINCENT, *On the identification of symmetric quadrature rules for finite element methods*, Comput. Math. Appl., 69 (2015), pp. 1232–1241, doi:10.1016/j.camwa.2015.03.017.

[37] H. C. Yee and B. Sjögreen, *Designing adaptive low-dissipative high order schemes for long-time integrations*, in Turbulent Flow Computation, Kluwer Academic Publishers, 2002, pp. 141–198, doi:10.1007/0-306-48421-8_5.

[38] H. C. Yee, M. Vinokur, and M. J. Djomehri, *Entropy splitting and numerical dissipation*, J. Comput. Phys., 162 (2000), pp. 33–81, doi:10.1006/jcph.2000.6517.

[39] L. Zhang, T. Cui, and H. Liu, *A set of symmetric quadrature rules on triangles and tetrahedra*, J. Comput. Math., 27 (2009), pp. 89–96.